ISIJ International, Vol. 59 (2019), No. 5, pp. 778–786

Effect of Nut Coke Addition on Physicochemical Behaviour of Pellet Bed in Ironmaking Blast Furnace

Dharm Jeet GAVEL,[1)]* Allert ADEMA,[2)] Jan Van Der STEL,[2)] Jilt SIETSMA,[1)] Rob BOOM[1)] and Yongxiang YANG[1)]

1) Department of Materials Science and Engineering, Delft University of Technology, Mekelweg 2, CD Delft, 2628 The Netherlands.
2) Research and Development, Tata Steel in Europe, CA IJmuiden, 1970 The Netherlands.

(*Received on August 21, 2018; accepted on December 19, 2018; J-STAGE Advance published date: February 14, 2019*)

One of the primary causes that limit the blast furnace productivity is the resistance exerted to the gas flow in the cohesive zone by the ferrous burden. Use of nut coke (10–40 mm) together with ferrous burden proves beneficial for decreasing this resistance. In present study, effect of nut coke addition on the olivine fluxed iron ore pellet bed is investigated under simulated blast furnace conditions. Nut coke mixing degree (replacement ratio of regular coke) was varied from 0 to 40 wt% to investigate the physicochemical characteristics of the pellet bed. Three distinct stages of bed contraction are observed and the principal phenomena governing these stages are indirect reduction, softening and melting. It is observed that nut coke mixing enhances the reduction kinetics, lowers softening, limits sintering and promotes iron carburisation to affects all three stages. In the second stage, the temperature and displacement range is reduced by 60°C and 24%, respectively upon 40 wt% nut coke mixing. Addition of nut coke exponentially increases the gas permeability (represented by pressure drop and S-value). A higher degree of carburisation achieved on the pellet shell (iron) is suggested to be the principal reason for decrease in the pellet melting temperature. The pellets softening temperature increases by approximately 4°C, melting and dripping temperature drops by 11°C and 12°C, respectively, for every 10 wt% nut coke addition. Consequently, the nut coke addition shortens the softening, melting and dripping temperature ranges, which shows improved properties of the cohesive zone.

KEY WORDS: blast furnace; ironmaking, nut coke; olivine pellets; softening; melting; carburisation; permeability.

1. Introduction

The ironmaking blast furnace is a counter-current reactor, in which reducing gases and solid raw material travel in opposite directions and exchange heat and mass efficiently. Hence, gas permeability is crucial at all levels of a blast furnace. About 25% of the total (furnace) pressure drop occurs in the cohesive zone, which is due to the softening and melting of ferrous raw materials.[1)] This zone of poor permeability has a negative impact on the productivity of the furnace. The gas permeability in the cohesive zone can be increased by mixing nut coke (10–40 mm) with the ferrous burden of pellets and/or sinter.[2–4)] Furthermore, nut coke addition to the ferrous raw material has beneficial effects on enhancing the shaft permeability, lowering thermal reserve zone temperature and improving burden softening-melting properties.[5)]

Some studies were already performed to understand the influence of nut coke addition on the ferrous burden. For example, Babich *et al.*[6)] reported the improvement in the shaft permeability, and therefore the furnace productivity was enhanced (1.5% to 2.5%) with the nut coke mixing (10–20 wt%). Mousa *et al.*[7–9)] revealed that nut coke addition enhances reduction kinetics to avoid 'reduction retardation' phenomena that occur at ~1 250°C due to the formation of fayalitic ($2FeO–SiO_2$) slag. The softening and melting of the ferrous burden are known to occur at high temperatures (1 250–1 450°C).[2,10)] Since these studies were performed at a relatively low temperature (below 1 250°C), no information was obtained on the effect of nut coke addition on the softening-melting temperatures. Additionally, when ferrous burden in the blast furnace reaches the cohesive zone, a massive pile of the burden rests on the top of raw material bed in this zone; inevitably this will have an impact on the physical properties of this area of the furnace.[11,12)] Since the loads were absent in those studies, test condition was not representative for the blast furnace and only rudimentary understanding was established.

Song[2)] incorporated the gases, temperature, and load conditions to simulate the burden behaviour inside the blast furnace. Former studies[2,13)] reported an increase in soften-

* Corresponding author: E-mail: d.j.gavel@tudelft.nl
DOI: https://doi.org/10.2355/isijinternational.ISIJINT-2018-580

ing and melting properties of the ferrous raw material when mixed charged with the nut coke. However, these studies did not include the variation in the added nut coke concentration (performed only with 20 wt%), and in-depth analysis is not provided.

Mostly, nut coke utilisation is driven by its generation during the coke making process. Despite being beneficial in the iron making process, nut coke is utilised in limited quantity (less than 23 wt%).[5] It was also reported elsewhere that nut coke addition may bring a negative impact on the overall gas permeability due to the regular coke layer thinning.[1,14]

Therefore, considering the idea of nut coke use as the replacement of regular coke, it is of utmost importance to understand its impact on the gas permeability, when regular coke layer is thinned due to the higher replacement ratios (more than 20 wt% of the regular coke). It is clear from the literature that there is a lack of fundamental understanding on the bed behaviour at high temperatures when nut coke is added in higher concentration as a replacement of the regular coke.

The present work aims to comprehensively evaluate and quantify the effects of nut coke addition (as a replacement of the regular coke) on the physicochemical property changes of the raw material (pellet) bed under simulated blast furnace conditions.

2. Materials and Method

2.1. Raw Materials

In the present study, commercially supplied olivine fluxed iron ore pellets with a size of 10–13 mm and nut coke with a size of 10–15 mm were used. The chemical analysis of the iron ore pellet sample, measured with XRF (X-ray fluorescence, Panalytical, Axios Max) is given in **Table 1**. The schematic of the sample arrangement inside the graphite crucible is shown in **Fig. 1**. Due to the graphite crucible size limitation, coke with a size of 20 to 25 mm was utilised as regular coke in the study. In the case of a sample bed without nut coke, a pellet layer was sandwiched between two regular coke layers (Fig. 1(a)), similar to the blast furnace layered structure. In the case of pellets mixed with nut coke, the regular coke was proportionally removed, and the coke layer becomes thinner (Fig. 1(b)). The regular coke was equally distributed between the top and bottom layers. To avoid critical thinning of the regular coke layer, experiments were performed up to a maximum of 40 wt% nut coke mixing, the replacement ratio of normal sized coke (called "nut coke concentration" in this study). Nut coke concentration was altered from 0 wt% to 40 wt% at the interval of 10 wt%. Experiments with each nut coke concentration were repeated twice to check the reproducibility. All experiments were carried out with a constant bed weight of coke (100 g) and pellets (500 g), which represents a coke ratio of 300 kg/t of hot metal (kg/tHM) in the blast furnace equivalent. And the blast furnace is supposed to operate with a PCI rate of 200 kg/tHM.

Table 1. Chemical analysis of the olivine fluxed iron ore pellets.

Species	Fe (total)	SiO_2	MgO	Al_2O_3	CaO	MnO	TiO_2	B_4 (Basicity)
Weight%	64.94	3.70	1.21	1.06	0.37	0.30	0.26	0.33

2.2. Experimental Conditions

The sample bed was heated in Reduction Softening and Melting (RSM) apparatus (**Fig. 2**), under simulated blast furnace conditions. During the experiments the thermal and gas profiles followed the previously measured conditions of an operating blast furnace,[15] and are given in **Table 2**. The mass flow controller of the respective gases (CO, CO_2, H_2 and N_2) were employed to control the gas flow rate. These gases were pre-mixed in the gas mixing station through mass flow controller then passed to the preheating furnace. Thereafter, the gas mixture flows upwards inside the reactor tube of the high temperature furnace from the inlet present at the bottom flange. Then, this mixture enters the crucible (height of 270 mm; internal diameter of 64 mm) from six holes and a nozzle located at the bottom of the crucible. For all experiments, a graphite nozzle of 5 cm high is fitted at the bottom of the crucible for the gas distribution. After interaction with sample, the gas chemistry was analysed and recorded.

The gas velocity inside the crucible is presented in Table 2. It is estimated by gas flow rate to the inner cross-sectional area of the crucible. In the blast furnace, the gas velocity is expected to change with the temperature and bed porosity.

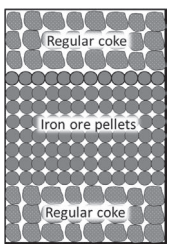

(a). Sample bed without nut coke.

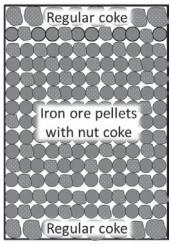

(b). Sample bed with mixed nut coke.

Fig. 1. Schematic of the sample bed arrangement inside the graphite crucible.

Table 2. Thermal and gas profile followed during the experiments.

Temperature range (°C)	Heating rate (°C/min)	CO (%)	CO_2 (%)	H_2 (%)	N_2 (%)	Gas flow rate (l/min)	Real gas velocity range* $x10^{-2}$ (m/sec)
20–400	7.0	0	0	0	100	5	2.7–6.2
400–600	5.0	25	20.5	4.5	50	15	18.6–24.1
600–950	5.0	30	15.5	4.5	50	15	24.1–33.7
950–1 050	1.2	33	12.0	5.0	50	15	33.7–36.5
1 050–1 550	5.0	42	0	8.0	50	15	36.5–50.3
1 550–20	5.0	0	0	0	100	5	16.8–2.7

*Assumed ideal gas behaviour in an empty crucible.

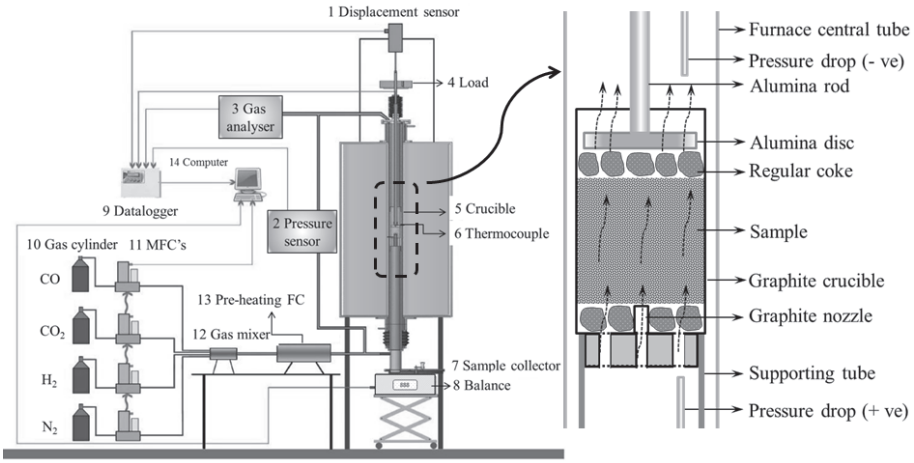

Fig. 2. Reduction Softening and Melting (RSM) apparatus.

The effect of temperature on the gas velocity is incorporated by assuming the ideal gas behaviour (Table 2). For the estimation of gas velocity, the crucible is considered empty (porosity, $\varepsilon = 1$). However, in the real blast furnace scenario, the bed porosity will be much less than 1 due to the presence of raw materials for iron production. Additionally, bed porosity will change with the temperature. Especially during softening and melting of the ferrous raw materials, the bed porosity will decrease dramatically. Consequently, the gas velocity will increase to result in higher pressure drop across the pellet bed. Furthermore, the mass flow rate of the total gas within the blast furnace may also change due to reduction reactions and gasification of coke. Inside the blast furnace, the pressure also changes along the height. All these should be taken into account when calculating the real local gas velocities.

During the tests, a load of 9.8 N/cm^2 was applied on the top of the sample bed (a total of 25 kg). To measure the sample bed contraction during softening and melting a displacement transducer (RDP, ACT2000C) was employed. The pressure difference across the sample bed was measured by a differential pressure transducer (Honeywell, KZ). Sample bed temperature was measured by the B-type thermocouple. The gas analysis, pressure drop and bed contraction were logged every 10 seconds and recorded in the datalogger (Atal, ATM05). More information about the experimental set-up, the crucible, the test procedure and conditions can be found in the references.[2,13] The thermodynamics software 'Factsage 7.0' was utilised to estimate the carbon concentration in the formed iron metal, produced from the above mentioned iron ore pellets.

3. Results and Discussion

3.1. Bed Displacement

The sample bed contraction as a function of temperature for all the experiments shows similar trends. **Figure 3** schematically illustrates the various stages of the bed contraction, and different parameters are defined in **Table 3**.

3.1.1. General Characteristics of Pellet Bed Contraction Behaviour

In the sample bed, three distinct stages of contraction occur (Fig. 3, Table 3). Under blast furnace conditions, the sample layer always evolves through these three stages.[11] Generally, the three principal phenomena responsible for bringing these three stages are indirect reduction, softening and melting. The complete list of different physicochemical phenomena which occur at these stages is given in **Table 4**.

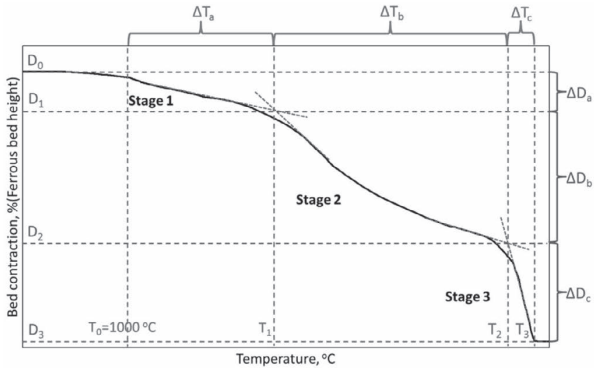

Fig. 3. Three stages of the sample bed contraction as a function of temperature.

In the first stage, marginal bed contraction occurs (Fig. 3). Stage 1 occurs primarily due to shrinkage of individual pellets as a result of gaseous (indirect) reduction. Pellets shrink due to the loss of the oxygen and sintering of gangue minerals.[16] Then the metallic iron forms during the complete reduction of the iron oxide (pellet). Due to topochemical reduction reactions the iron forms first at the pellet periphery and grows into a shell.[11,17] This thin iron shell becomes dense due to the sintering under the load which makes difficult for the reducing gases to reach the pellet core. Subsequently, with an increase in temperature, partially reduced pellet core (rich in FeO) and other oxides (SiO_2, CaO, MgO, and Al_2O_3), start to melt and forms a primary slag. This molten slag slowly fills up the micro-pores present in the pellet to cause softening start of the second stage of bed contraction and further hinders the reduction reactions to proceed. Along with softening, due to the close contact among the pellets, sintering takes place to result in bed contraction.[11,18] At the start of the second stage, the rate of displacement is high which later on decreases due to the depletion of the micropores (Fig. 3). Simultaneously, the pellet shell (iron) carburises by the CO gas[19] and carbon

from regular coke present in the close vicinity.[20] Due to the close contact between the pellets and regular coke at the layer interface, the iron carburisation degree is large. Based on the carburisation degree achieved in the iron shell, melting occurs. Consequently, the pellet deforms and melting start to mark the start of stage 3. As the first layer of pellets melts away, the regular coke layer moves to the next pellet layer to carburise and thereafter melting proceeds. This continues layer-wise till all the pellets get molten and drained out. Because of the shell melting, the liquid present at the core gets released, formed before or during the shell carburisation. Once this liquid (metal and slag) starts to flow over the coke, metal rich portion picks up the carbon and slag (rich in FeO) is reduced first (direct reduction) and subsequently carburised. At the end of stage 3 due to the draining of liquid, the bed height becomes constant.

Table 3. Parameters of the sample bed contraction.

Symbol	Notion	Unit
Stage 1	Individual pellet shrinkage due to reduction	–
Stage 2	Softening, sintering, and iron carburisation	–
Stage 3	Melting of ferrous burden and melt dripping (molten iron and slag)	–
T_0	=1 000°C, This temperature is defined as end temperature of the thermal reserve zone in the blast furnace,[19] and is taken as 1 000°C.	°C
T_1	First stage end temperature. Identified by the intersection point of tangents drawn to stage 1 and stage 2 behaviour. T_1 represents the start of pellet bed softening.	°C
T_2	Second stage end temperature. Identified by the intersection point of tangents drawn to stage 2 and stage 3 behaviour. T_2 represents the start of individual pellet melting in the bed.	°C
T_3	Third stage end temperature. Identified as the point after which no further bed contraction occurs.	°C
ΔT_a	(T_1-T_0), the temperature interval between the thermal reserve zone and the end of stage 1.	°C
ΔT_b	(T_2-T_1), the temperature interval of stage 2. Softening temperature range.	°C
ΔT_c	(T_3-T_2), the temperature interval of stage 3. Melting and dripping temperature range.	°C
D_0	Sample layer contraction at the start of an experiment (= 0%).	%
D_1	Bed contraction at the end of stage 1. Identified by the intersection point of tangents drawn to stage 1 and stage 2.	%
D_2	Bed contraction at the end of stage 2. Identified by the intersection point of the tangents drawn to stage 2 and stage 3.	%
D_3	Bed contraction at the end of stage 3. Identified as the point after which no further contraction occurs.	%
ΔD_a	(D_1-D_0), bed displacement in stage 1, occurs due to indirect reduction.	%
ΔD_b	(D_2-D_1), bed displacement in stage 2, occurs due to pellet softening.	%
ΔD_c	(D_3-D_2), bed displacement in stage 3, occurs due to melting and draining.	%

Table 4. Physicochemical phenomena and stages of the pellet bed contraction.

Physicochemical Phenomena	Stage 1	Stage 2	Stage 3
Swelling of individual pellets	✓	–	–
Indirect reduction (gaseous reduction)	✓	✓	–
Metal (iron) formation	✓	✓	–
Shrinking of individual pellets	✓	✓	–
Softening of the pellets	–	✓	–
Sintering of the pellets	–	✓	–
Pellet Fe shell carburisation (in solid state)	–	✓	✓
Pellet deformation and collapse	–	–	✓
Iron carburisation (in liquid state)	–	–	✓
Pellet melting and dripping	–	–	✓
Direct reduction	–	–	✓

3.1.2. Effect of Nut Coke Addition on Pellet Bed Contraction

The sample bed contraction recorded as a function of temperature is shown in **Fig. 4**. Influence of nut coke addition on the sample bed shrinkage is discussed in detail in the sections below.

(1) Effect of Nut Coke Addition on Stage 1 Behaviour

Iron ore pellet swelling is known to occur around 1 000°C, which is inside the first stage.[11,21,22] However, in the present case due to the load (9.8 N/cm^2) on the top of sample bed, limited swelling in the sample bed is observed (Fig. 4). The point T_1 which represents the start of pellet softening, shifts to a higher temperature as a result of an increase in the reduction degree with nut coke addition. Consequently, less liquid (slag) formation and limited sintering among the pellets occur in bed mixed with more nut coke (**Figs.** 4 and **5**). Additionally, due to extended stage 1 regime, the indirect reduction of the pellets further enhances. The first stage end temperature (T_1) linearly increases from 1 149°C to 1 165°C up to 40 wt% nut coke addition (Fig. 5). T_1 increases by

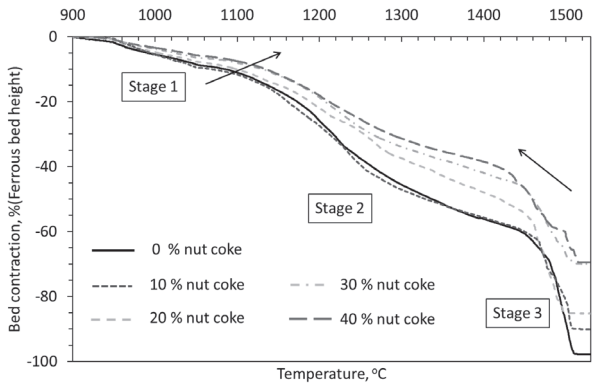

Fig. 4. Effect of nut coke addition on the sample bed contraction.

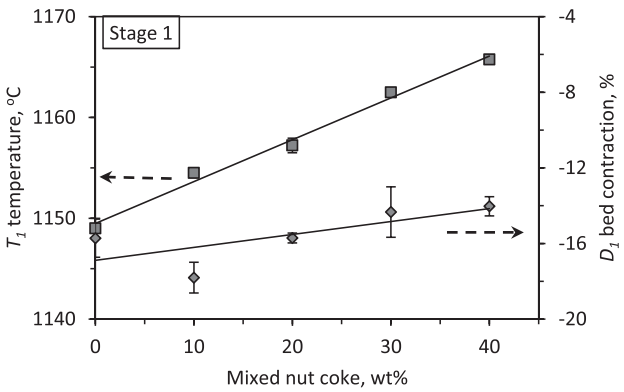

Fig. 5. Effect of nut coke mixing on stage 1 of bed contraction (individual pellet shrinkage) and start of pellet softening.

~4°C for every 10 wt% nut coke addition in the pellet bed.

Despite higher reduction achieved in the presence of nut coke, the sample bed contraction degree decreases marginally, *i.e.* by ~2% for 40 wt% nut coke mixing (Fig. 5). Additionally, the variance in the first stage displacement is observed to be high, which is possible due to the shape factor of the added material in the bed. Although the particle size is in close range, the shape of the sample varies, especially for the nut coke. This could bring fluctuation in the first stage of bed contraction. Now considering the trend and magnitude of the variance in the measured data for two experiments, a linear relationship is assumed between the nut coke addition and the first stage of displacement.

(2) Effect of Nut Coke Addition on Stage 2

Nut coke addition has a substantial effect on stage 2 (**Figs.** 4 and **6**), which is also known as softening stage. The stage 2 end temperature (T_2), which represents the start of individual pellet melting and collapse, decreases linearly from 1 480°C to 1 436°C upon the addition of 40 wt% nut coke in the pellet bed (Fig. 6). Consequently, the temperature difference between the start (T_1) and end of second stage (T_2) decreases drastically, *i.e.* by 15°C with every 10 wt% nut coke addition in the pellet bed. The bed contraction in stage 2 (D_2) decreases linearly from 70% to 44% (Fig. 6). D_2 decreases by 6.5% for every 10 wt% nut coke mixing in the pellet bed.

One of the primary reasons for the bed contraction in the second stage is the sintering among the pellets.[11] Sintering not only results in higher bed contraction but also slows down reducing gases in reaching the unreduced portion of the pellets which melts ($2FeO.SiO_2$) along with gangue at a relatively low temperature and causes reduction retardation.[7,23] These in-situ melt formation decreases the strength of the pellet to cause the softening. However, under mixed charge condition, nut coke hinders the sintering among the pellets and also facilitates the gases with a high reduction potential to reach the pellet core so as to minimize the reduction retardation.[7] Consequently, the pellet strength and softening temperature increases.

Furthermore, direct contact between coke and pellet (shell iron) enhances the kinetics of iron carburisation and thus decreases the melting point of the pellet shell (Fe–C). As a result, a decrease in starting temperature of the pellet melting is observed (Figs. 4 and 6). It is also evident from the iron-carbon phase diagram that with the increase in the carbon concentration in iron, the melting temperature (liquidus) decreases.[24] The kinetics for the reduction reactions, the rate of metal (iron) formation and iron carburisation are observed to enhance with nut coke addition in the pellet bed.

(3) Effect of Nut Coke Addition on Stage 3

Stage 3 ends with melting and dripping of the ferrous burden, when maximum possible bed contraction is achieved. The stage 3 end temperature (T_3) is observed in the range between 1 505°C to 1 520°C for the pellets mixed with and without nut coke (**Figs.** 4 and **7**). It shows that T_3 increases with the nut coke addition in the pellet bed. Due to the higher reduction degree achieved on the pellets, a thicker iron shell formed.[18] This shell takes comparatively longer time and higher temperature for carburisation, melting and dripping.

As a result of nut coke mixing, the initial sample bed height (pellets + nut coke) increases. Now during the experiment, the iron ore pellets melt and drain out to leave the unconsumed nut coke in the sample bed. Consequently, the final bed displacement (D_3) decreases with the nut coke addition. A linear relationship is found between D_3 and nut coke addition (Fig. 7).

(4) Bed Displacement and Temperature Range

From **Figs. 8**(a) and 8(b), it can be seen that the effect of nut coke addition is most significant in the stage of softening (second stage). Temperature range for the first (ΔT_a) and third (ΔT_c) stages increases with the nut coke mixing (Fig. 8(a)). Nut coke being a source of carbon placed in close vicinity of the pellets (iron oxide) enhances reduction kinetics. The second stage temperature range strongly depends on the kinetics of reduction and carburisation of the pellet shell (iron). Nut coke brings higher carburisation on the freshly reduced iron, present at the pellets periphery. This results in the earlier melting of the shell (Fe–C) to shorten the second stage temperature range (ΔT_b) by 60°C upon 40 wt% nut coke addition. In the softening stage, the nut coke hinders the direct contact between the pellets and therefore slows down sintering among the other pellets to decrease the bed contraction. Nut coke also acts as a skeleton in the softening pellet bed to resist the load on the top. Consequently, in the second stage, the bed displacement decreases substantially, *i.e.* by 24% upon 40 wt% nut coke addition (Fig. 8(b)).

In the presence of nut coke, ΔT_a increases due to the delay in the softening of the pellets, which is induced by the less liquid slag formation and limited sintering among the pellets

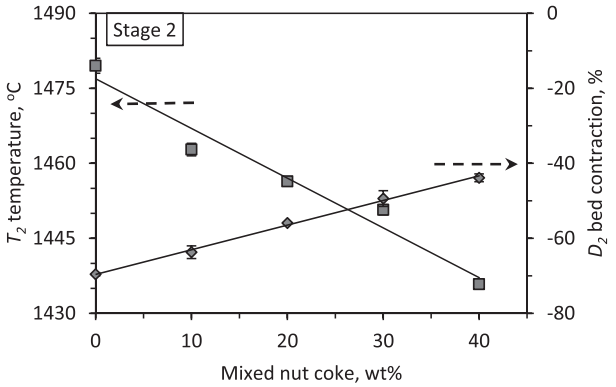

Fig. 6. Effect of nut coke addition on stage 2 of bed contraction at the end temperature of softening.

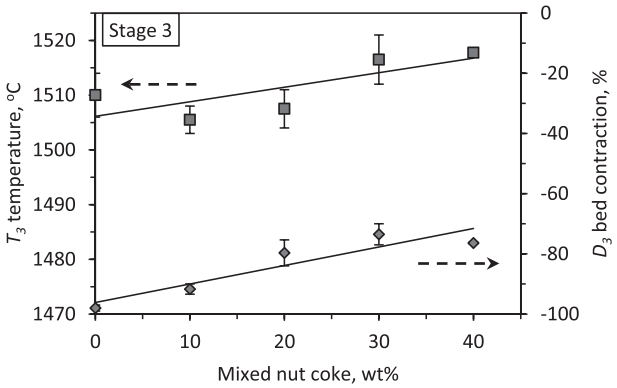

Fig. 7. Effect of nut coke mixing on the third stage of bed contraction at the end temperature of the melting.

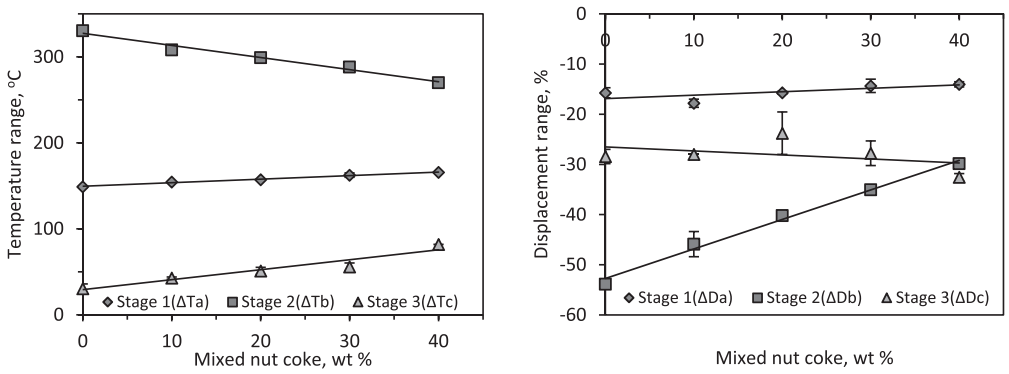

(a). Temperature ranges of three stages. (b). Bed displacement of three stages.

Fig. 8. Effect of nut coke on bed displacement and temperature ranges of different stages.

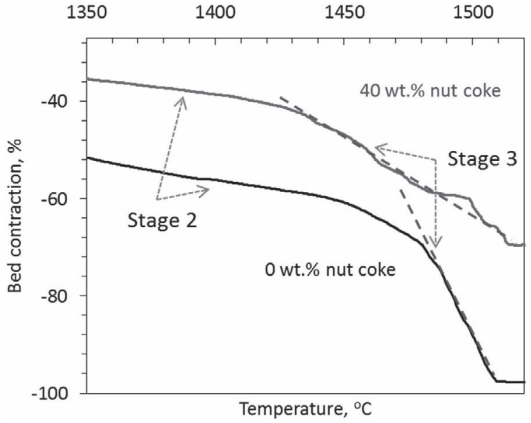

Fig. 9. Effect of nut coke addition on the slope of the third stage of bed contraction (melting and dripping).

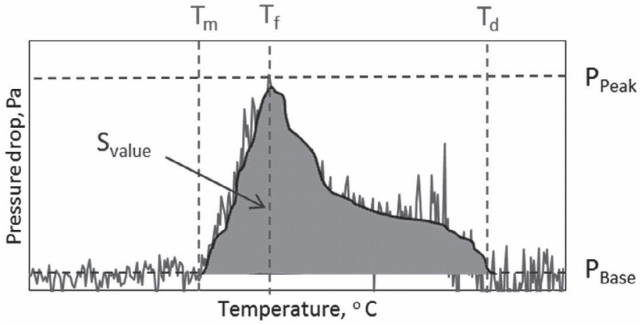

Fig. 10. Typical pressure drop curve during softening melting and dripping of the sample.

(Fig. 8(b)). And, in the third stage, displacement occurs due to the melting and draining of ferrous material from the bed. Therefore, before reaching the third stage, due to softening and sintering the maximum possible compaction has already been achieved in the bed. Now with the nut coke addition, in the third stage, a marginal increase in the bed displacement was observed. The higher utilisation of added nut coke in the bed for iron carburisation and reduction of FeO rich slag in the liquid state would bring this change in the third stage.

As discussed earlier, a thicker layer of iron forms at the pellet periphery in the presence of nut coke.[18] To carburise and melt this thick iron (Fe–C) layer more time and higher temperature range are required. Therefore in the third stage for only ~30% displacement (Fig. 8(b)), a relatively longer temperature interval means a sluggish rate of bed contraction (**Figs.** 4 and **9**). Slower rate of bed contraction is evident from the third stage slopes, which is compared for two extreme cases in Fig. 9. Additionally, nut coke being solid at the time of pellet melting supports the bed structure to slow down the collapse.

3.2. Gas Permeability

3.2.1. General Characteristics of Gas Permeability Across the Pellet Bed

A steady pressure difference between the gas inlet and outlet means that a large density of pores are available in the sample bed for the gas flow. As described in the earlier section, due to the liquid formation pellet softening occurs (second stage of bed contraction). The formed liquid is mostly entrapped in the pellet core and in the micro-pores present on the pellet. As the iron shell melts and breakout occurs, this liquid slag and metal comes out and starts to fill up the interstitial voids. Consequently, the pressure drop increases drastically across the sample bed. Therefore, the temperature at which the pressure drop start to increase sharply from the base value (P_{Base}) is considered as the melting temperature for the sample bed (T_m) (**Fig. 10**). After that, flowing liquid floods the bed to cause the maximum pressure drop P_{peak} across the bed at T_f temperature. Then the downward flow of the melt starts and as a result, new space is available for the gas flow. Therefore, the pressure drop decreases after the flooding point (T_f).

Now in the case of pellet bed without nut coke, the pressure drop continues to remain high due to the layer wise melting and presence of liquid in the bed. Once this liquid drains out sufficiently, the pressure drop recovers back to the base value (P_{Base}, Fig. 10). The temperature at which the pressure drop returns to the base value is defined as the dripping point (T_d).

3.2.2. Effect of Nut Coke on Gas Permeability

Nut coke addition affects the gas permeability and key temperatures (T_m, T_f and T_d) of the sample bed (**Fig. 11**). The pressure drop curves recorded during the experiments with and without nut coke is shown in Fig. 11.

The principal observed effect of nut coke addition in the pellet bed are quantified and discussed in the section below.

(1) Pressure Drop and S-value

The pressure difference between the gas inlet and outlet through the packed bed increases due to the resistance provided by the ferrous raw material during softening and

melting phenomena.[10] Therefore, the complete area under the pressure drop curve is a measure of total resistance provided by the raw material during the softening and melting phenomena. It is represented as '*S-value*' (**Table 5** and Fig. 10). At the point of highest pressure drop (T_f), a low density of voids are available for the gas flow. Thus, the higher the magnitude of pressure drop, the lower number of pores available for the gas flow (Figs. 10 and 11).

The peak pressure drop (P_{peak}) and *S-value* decrease with the nut coke addition (**Figs. 12**(a) and 12(b)). Nut coke remains solid under the blast furnace cohesive zone temperature conditions. These provide additional micro (on nut coke), and macro (interstitially) pores for the gas flow to result in a comparatively lower pressure drop during the melting process (Fig. 12(a)). Melting and breakout of ferrous raw material occur in the third stage of bed contraction. As evident from stage 3 slope (Fig. 9), the rate of bed contraction decreases with the nut coke addition in the bed. Thus at any instant, the melt volume is comparatively small to fill up the open pores. Therefore a lower pressure drop is observed in the pellet bed mixed with the nut coke.

The decreasing trend of the peak pressure drop (P_{peak}) height with the nut coke addition is evident from Figs. 11 and 12(a). A large variance suggests that the internal sample arrangement also has a strong influence on the pressure drop peak (P_{peak}) height (Fig. 12(a)). Nevertheless, the permeability (represented by P_{peak} and *S-value*) was found to improve exponentially with the nut coke addition (Fig. 12).

(2) Effect of Nut Coke on Pellet Bed Melting, Flooding and Dripping Temperature

The temperatures of the pellet bed melting (T_m), flooding (T_f) and dripping (T_d) are examined according to the definition presented in Fig. 10 and Table 5. T_m, T_f and T_d decrease linearly by ~4°C, 6°C, and 11°C, respectively for every 10 wt% nut coke addition in the pellet bed (**Fig. 13**). The range between the bed melting temperature (T_m) and dripping temperature (T_d) decreases by 28°C with the addition of up to 40 wt% nut coke.

The prime cause of the decrease in pellet bed melting

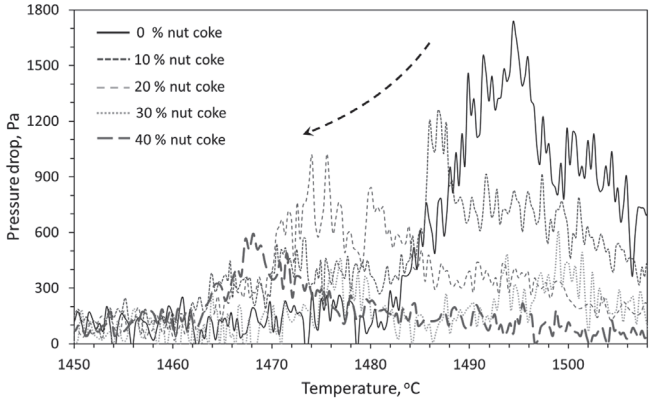

Fig. 11. Effect of nut coke addition on the gas permeability (represented by the pressure drop).

Table 5. Process parameters of pressure drop in the sample bed.

Symbol	Notion	Unit
T_m	The melting point of the sample bed, the temperature at which pressure drop in the bed starts to increase steeply.	°C
T_f	The flooding point, the temperature at which the pressure drop reaches the maximum and the melt starts dripping out of the bed.	°C
T_d	The dripping point, the temperature at which pressure drop value reaches back to the base value as before the softening and melting.	°C
P_{Base}	The base value of pressure drop before melting phenomenon.	Pa
P_{Peak}	The peak value of pressure drop, the maximum pressure drop value during softening and melting.	Pa
S_{value}	The area under the pressure drop curve, being a measure of resistance offered by the sample to gas flow during softening and melting.	kPa.°C

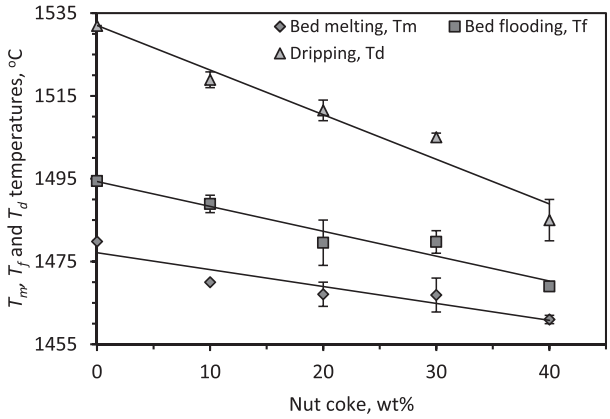

Fig. 13. Effect of nut coke addition on the bed melting (T_m), flooding (T_f) and dripping (T_d) temperature deduced from the pressure drop curve.

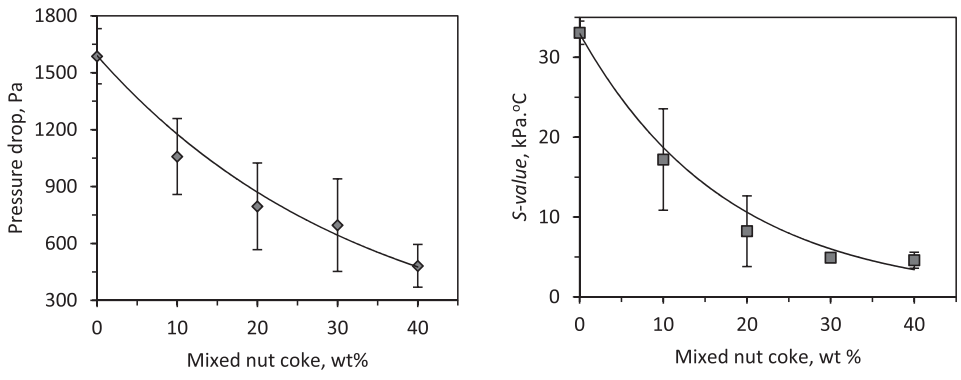

(a) (b)

Fig. 12. Effect of nut coke addition on (a). Pressure drop peak (P_{peak}) and (b). S-value.

temperature (T_m) is the high degree of iron carburisation achieved on the iron shell induced by the presence of nut coke. The nut coke promotes the reduction kinetics and carburisation of the pellets due to its larger surface area and close contact with the pellets.[18)]

3.3. Effect of Nut Coke Addition on Pellet and Bed Melting

In the case of sample mixed with nut coke, the pellet bed (bulk) melting temperature (T_m, Table 5) is different from the individual pellet melting (T_2, Table 3). The stage 2 end temperature (T_2) represents the start of the individual pellet melting, and the bed melting (T_m) denotes the temperature at which the melt has spread to the bed to pose a substantial resistance to the gas flow. As explained earlier, nut coke remains solid at the time of pellet softening and melting to provide interstitial space (macro-pores) to accommodate the deformation and melts from pellets. As a result, the temperature difference between T_2 and T_m arise (**Fig. 14**). A linear relationship is found between the nut coke addition and the difference between these two melting temperatures (T_m and T_2). The difference in melting temperatures increases by 6°C for every 10 wt% nut coke addition.

3.4. Effect of Nut Coke on Softening and Melting Temperature Range

In the blast furnace, the cohesive zone starts with softening of the ferrous burden and ends with the dripping of the liquid melt.[19)] In the related temperature range, the burden is known to exert substantial resistance against the gas flow. Therefore, it is desired in the blast furnaces to have this zone as narrow as possible.[10)] During the experiments under simulated blast furnace conditions, the cohesive zone temperature range is represented by the difference between the starting temperature of the softening stage (T_1) and dripping temperature (T_d). It is observed from the experiments that this temperature interval decreases substantially, *i.e.* up to 64°C upon 40% nut coke addition. The T_1 and T_d temperatures along with the difference are plotted in **Fig. 15**.

3.5. Effect of Nut Coke on Iron Carburisation

It is well known that carburisation can lower the melting temperature of the iron-carbon alloy below 4.3 wt%. Under blast furnace conditions, the iron forms at the pellet periphery and is carburised by the CO gas[19)] and carbon (nut coke) present in the close vicinity.[20)] At a certain temperature, the pellet shell (iron) melts due to the increase in the carburisation degree. As a result, a breakout occurs to release liquid from the pellet core. Mixing the nut coke into ferrous burden results in a larger interface area of solid carbon with the pellets. Also, the relatively high permeability of the burden (voidage) creates a large gas-pellet interfacial area. Therefore, the carburisation degree of the pellet shell is expected to be higher with a burden of nut coke mixed charge. Correspondingly, pellet melting (T_2) and dripping (T_d) temperature will be lower with higher nut coke amount.

It is generally referred that under the blast furnace conditions the reactions evolve close to the equilibrium.[19)] Therefore, the carbon present at the point of melting can be estimated using the iron-carbon equilibrium phase diagram. If we assume the pellet melting temperature (T_2) to be the liquidus temperature of the iron-carbon alloy, the equilibrium concentrations of the carbon in solidus and liquidus iron at T_2 can be estimated using Factsage 7.0 (**Fig. 16**). Notably, a steep increase in the liquidus carbon concentration is noted from 0.7 to 1.3 wt% upon 40 wt% nut coke addition (Fig. 16). As it is shown, the increase of carbon concentration leads to the linear decrease of pellet melting temperature.

Theoretically, once the carbon concentration of the pellet shell distributes within this range, the shell melting occurs.

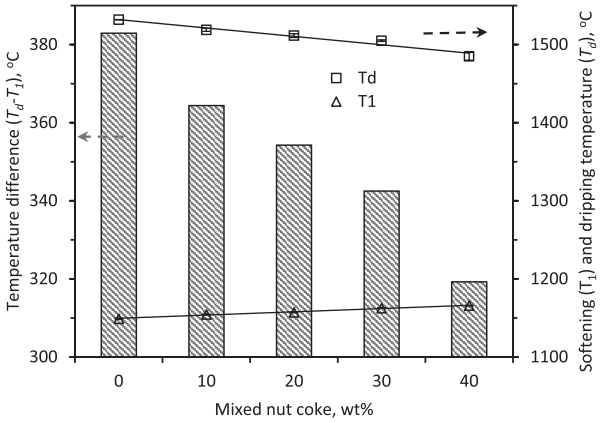

Fig. 15. Effect of nut coke addition on the softening and dripping temperatures (represents the cohesive zone temperature range in the blast furnaces).

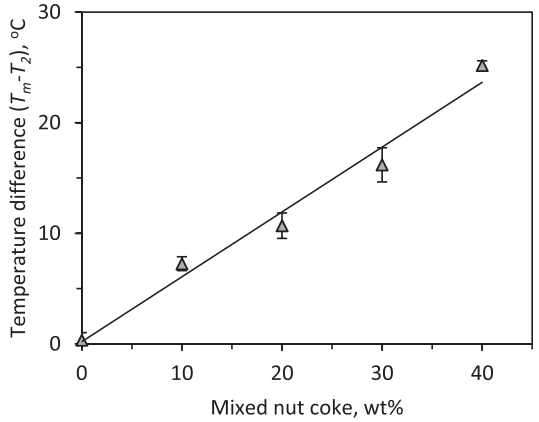

Fig. 14. Difference between the pellet bed melting temperature (T_m) and individual pellet melting temperature (T_2).

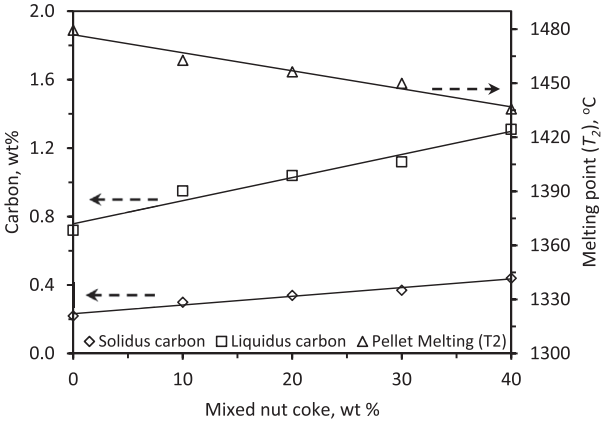

Fig. 16. Estimated effect of nut coke addition on the solidus and liquidus carbon concentration by using FactSage software.

Table 6. Relationship summary on the effect of nut coke addition in the pellet bed.

Parameters	Unit	Relationship	Equation x= nut coke concentration (wt%)	R^2
Stage 1 temperature (T_1)	°C	Linear	0.42x + 1 150	0.99
Stage 1 displacement (D_1)	%	Linear	0.07x − 17	0.53
Stage 2 temperature (T_2)	°C	Linear	−0.99x + 1 477	0.96
Stage 2 displacement (D_2)	%	Linear	0.66x − 70	1.00
Stage 3 temperature (T_3)	°C	Linear	0.27x + 1 506	0.59
Stage 3 displacement (D_3)	%	Linear	0.61x − 96	0.85
Bed melting temperature (T_m)	°C	Linear	−0.41x + 1 477	0.87
Flooding temperature (T_f)	°C	Linear	−0.60x + 1 494	0.94
Dripping temperature (T_d)	°C	Linear	−1.08x + 1 532	0.96
(T_m−T_2)	°C	Linear	0.59x + 0.20	0.98
Pressure drop peak (P_{peak})	Pa	Exponential	$1\,590e^{-0.03x}$	0.97
Permeability (*S-value*),	kPa.°C	Exponential	$33e^{-0.06x}$	0.93

Moreover, it can also be predicted that to have sufficient fluidity for the deformation and liquid flow, the present carbon concentration might be close to its liquidus value rather than to the solidus concentration at the time of pellet melting (T_2).

Based on the series of experiments, the effect of nut coke addition on the various process parameters were studied in detail. These key relationships are summarised in **Table 6**. As discussed earlier, for temperature and displacement parameters the effect of nut coke addition is linear either with the positive or negative slope. Gas permeability (P_{peak} and *S-value*) is observed to increase exponentially with the nut coke addition.

4. Conclusions

The impact of nut coke addition (0–40 wt%) on an olivine fluxed iron ore pellet bed was studied in a reduction softening and melting (RSM) apparatus. Based on the series of experiments, the following conclusions can be drawn.

(1) Three distinct stages of bed contraction were observed during the pellets heating under simulated blast furnace conditions. In the first stage, indirect reduction of the iron ore pellet takes place. Sintering, softening and carburisation of the iron shell evolves in the second stage. Thereafter in the third stage, pellet melting and dripping occurs.

(2) Nut coke mixing with the iron ore pellet affects all three stages. The second stage get affected the most, which is shortened due to the enhanced reduction kinetics, limited sintering, lower softening and high degree of carburisation occurred on the pellet shell (iron). In the second stage, the bed displacement and temperature linearly decrease from 70% to 44% (6.5% per 10 wt% nut coke mixing) and 1 480 to 1 436°C (11°C per 10 wt% nut coke mixing), respectively by mixing of 40 wt% nut coke.

(3) The pellet bed melting (T_m), flooding (T_f) and dripping (T_d) temperatures, decrease linearly by 19°C, 25°C and 47°C, respectively upon 40 wt% nut coke addition.

(4) The cohesive zone temperature range (T_1 to T_d) shortens by 64°C by 40 wt% of nut coke addition.

(5) The nut coke addition exponentially increases the gas permeability (represented by pressure drop peak and *S-value*) in the pellet bed (examined up to 40 wt% as replacement of regular coke).

Acknowledgement

This research was carried out under project T41.5.13490 in the framework of the research program of the Materials innovation institute (M2i). The project was conducted at the Department of Materials Science and Engineering (MSE) of the Delft University of Technology in the Netherlands.

REFERENCES

1) M. Geerdes, R. Chaigneau, I. Kurunov, O. Lingiardi and J. Ricketts: Modern Blast Furnace Ironmaking: An Introduction, IOS Press BV, Amsterdam, (2015), 87.
2) Q. Song: Ph.D. thesis, Delft University of Technology, (2013), 137, https://doi.org/10.4233/uuid:c774c99c-2f40-48bb-852a-c8cb4e77d7d2, (accessed 2018-10-01).
3) T. Kon, S. Natsui, S. Matsuhashi, S. Ueda, R. Inoue and T. Ariyama: *Steel Res. Int.*, **84** (2013), 1146.
4) S. Matsuhashi, H. Kurosawa, S. Natsui, T. Kon, S. Ueda, R. Inoue and T. Ariyama: *ISIJ Int.*, **52** (2012), 1990.
5) D. J. Gavel: *Mater. Sci. Technol.*, **33** (2017), 381.
6) A. Babich, D. G. Senk, S. L. Yaroshevskiy, N. S. Chlaponin, V. V. Kochura and A. V. Kuzin: Proc. 3rd Int. Conf. on Process Development in Iron and Steelmaking (Scanmet III), MEFOS, Lulea, (2008), 227.
7) E. Mousa, D. Senk and A. Babich: *Steel Res. Int.*, **81** (2010), 706.
8) E. A. Mousa, D. Senk, A. Babich and H. W. Gudenau: *Ironmaking Steelmaking*, **37** (2010), 219.
9) E. A. Mousa, A. Babich and D. Senk: *ISIJ Int.*, **51** (2011), 350.
10) B. Nandy, S. Chandra, D. Bhattacharjee and D. Ghosh: *Ironmaking Steelmaking*, **33** (2006), 111.
11) J. Sterneland and A. K. Lahiri: *Ironmaking Steelmaking*, **26** (1999), 339.
12) A. A. El-Geassy, M. I. Nasr and M. H. Khedr and K. S. Abdel-Halim: *ISIJ Int.*, **44** (2004), 462.
13) Q. Song, Y. Yang and R. Boom: *Baosteel Tech. Res.*, **9** (2015), 8.
14) K. Ichikawa, J. Ishii, S. Watakabe, M. Sato, N. Oyama and H. Matsuno: Proc. METEC and 2nd European Steel Technology and Application Days (ESTAD), Steel Institute VDEh, Düsseldorf, (2015), 1.
15) R. Chaigneau, K. Sportel, J. Trouw, R. Vos and J. Droog: *Ironmaking Steelmaking*, **24** (1997), 461.
16) G. Wang, Q. Xue and J. Wang: *Thermochim. Acta*, **621** (2015), 90.
17) M. Iljana, A. Kemppainen, T. Paananen, O. Mattila, E. P. Heikkinen and T. Fabritius: *ISIJ Int.*, **56** (2016), 1705.
18) D. J. Gavel, Q. Song, A. Adema, J. V. D. Stel, J. Sietsma, R. Boom and Y. Yang: *Ironmaking Steelmaking*, (2018), https://doi.org/10.1080/03019233.2018.1510873.
19) A. K. Biswas: Principles of Blast Furnace Iron Making - Theory and Practice, Cootha Publishing House, Brisbane, (1981), 288.
20) K. Nagata, R. Kojima, T. Murakami, M. Susa and H. Fukuyama: *ISIJ Int.*, **41** (2001), 1316.
21) T. Sharma, R. C. Gupta and B. Prakash: *ISIJ Int.*, **32** (1992), 812.
22) F. W. Frazer, H. Westenberger, K. H. Boss and W. Thumm: *Int. J. Miner. Process.*, **2** (1975), 353.
23) T. Bakker: Ph.D. thesis, Delft University of Technology, (1999), 251, http://resolver.tudelft.nl/uuid:67eb1cc0-fd0f-443f-87a4-96e59c114af5, (accessed 2018-10-01).
24) O. K. Goldbeck: Iron-Binary Phase Diagrams, Springer, Berlin, (1982), 23.